

## THE MODEL DEPENDENCE OF SOLAR ENERGETIC PARTICLE MEAN FREE PATHS UNDER WEAK SCATTERING

G. QIN,<sup>1</sup> M. ZHANG,<sup>1</sup> J. R. DWYER,<sup>1</sup> H. K. RASSOUL,<sup>1</sup> AND G. M. MASON<sup>2</sup>

Received 2004 May 24; accepted 2005 March 9

### ABSTRACT

The mean free path is widely used to measure the level of solar energetic particles' diffusive transport. We model a solar energetic particle event observed by *Wind* STEP at 0.31–0.62 MeV nucleon<sup>-1</sup>, by solving the focused transport equation using the Markov stochastic process theory. With different functions of the pitch angle diffusion coefficient  $D_{\mu\mu}$ , we obtain different parallel mean free paths for the same event. We show that the different values of the mean free path are due to the high anisotropy of the solar energetic particles. This makes it problematic to use just the mean free path to describe the strength of the solar energetic particle scattering, because the mean free path is only defined for a nearly isotropic distribution. Instead, a more complete function of pitch angle diffusion coefficient is needed.

*Subject headings:* diffusion — interplanetary medium — solar wind

### 1. INTRODUCTION

Pitch-angle scattering by magnetic fluctuations is an essential transport mechanism of solar energetic particles (SEPs). The particles' parallel mean free path can be derived from the pitch angle diffusion coefficient (the quasi-linear theory [QLT], Jokipii 1966; Hasselmann & Wibberenz 1968; Earl 1974) for the particles with a nearly isotropic pitch-angle distribution. Parker (1965) obtained a diffusion equation of particle transport for applications such as the study of cosmic-ray modulation. However, considering SEPs, the focused transport equation is needed because the particles experience strong magnetic focusing near the sun (Parker 1963; Roelof 1969; Ng & Reames 1994). To describe the SEPs' scattering by the magnetic fluctuations, the focused transport equation can be solved to model the observed intensity and anisotropy profiles. Since it is very difficult to solve the equation analytically, numerical solutions have been provided (e.g., Ng & Wong 1979; Schlüter 1985; Ruffolo 1991; Kocharov et al. 1998). Kocharov et al. (1998) found different intensity profiles for isotropic and anisotropic pitch-angle scattering under a nominally similar mean free path. Note that previous authors have not studied how the different pitch angle diffusion models used in their numerical methods affect the simulation results by modeling observations.

However, it is known that under some conditions the SEPs have high anisotropy during the initial phase of a solar event (e.g., Schulze et al. 1977; Mason et al. 1989; Torsti et al. 2004). From the numerical calculations of the focused transport equation, Mason et al. (1989) showed that the particles' anisotropy increases dramatically as  $\lambda_{\parallel}$  increases. They got large values of the parallel mean free paths ( $\gtrsim 1$  AU) for some impulsive SEP events by fitting the numerical solutions of the transport equation to the spacecraft observations. Torsti et al. (2004) reported that in some events when SEPs propagate under weak scattering conditions, very large parallel mean free paths,  $\lambda_{\parallel} \geq 10$  AU, are obtained from fits to these events. With test-particle orbit-tracing simulations and theoretical calculations, Qin et al. (2004) showed that the strong magnetic focusing effect can make all the pitch-

angle distribution of SEPs become a beamlike distribution immediately after they are released near the Sun.

In this article we model an impulsive SEP event observed by *Wind* STEP (von Rosenvinge et al. 1995) with a focused transport equation, which is solved by a method of Markov stochastic process simulation (Zhang 1999, 2000). We obtain mean free paths by fitting numerical results to the spacecraft data. The STEP instrument is a time-of-flight mass spectrometer, capable of measuring ions from several tens of keV nucleon<sup>-1</sup> up to several MeV nucleon<sup>-1</sup>. The data are measured in eight azimuthal bins. In order to calculate pitch angles, *Wind* MFI magnetic field data (Lepping et al. 1995) are used. For the 0.5 MeV nucleon<sup>-1</sup> SEP data we study we can compute the Compton-Getting corrections (Dwyer et al. 1997) for the event-averaged pitch angle distribution function using *Wind* SWE (Ogilvie et al. 1995) solar wind velocity data, but we have difficulty computing the Compton-Getting corrections for the anisotropy time profile because of the low time resolution of the data. Furthermore, because the particle speed is much greater than the solar wind speed, the Compton-Getting corrections we get are smaller than the data's error bar, so in this work we ignore the Compton-Getting corrections. We concentrate on the investigation of how the pitch angle diffusion models can affect the determination of the mean free path. We obtain significantly different mean free paths from the different models of the pitch angle diffusion coefficients. Furthermore, we discuss the validity of using the mean free path to describe the transport of SEP events for which their anisotropy is high. Note that we get similar results for different species and energy, but as an example, in this paper we only show the results from 0.31–0.62 MeV nucleon<sup>-1</sup> He.

### 2. APPROACH AND METHODS

We model the transport of the *Wind* STEP energetic solar particle events (von Rosenvinge et al. 1995) with the numerical simulations using the Markov stochastic process theory (Zhang 1999, 2000). In our model, the focused transport equation in solar wind frame can be written as (Roelof 1969)

$$\frac{\partial f}{\partial t} + \mu v \frac{\partial f}{\partial z} - \frac{v(1-\mu^2)}{2B} \frac{\partial B}{\partial z} \frac{\partial f}{\partial \mu} - \frac{\partial}{\partial \mu} \left( D_{\mu\mu} \frac{\partial f}{\partial \mu} \right) = q(z, \mu, t), \quad (1)$$

<sup>1</sup> Department of Physics and Space Sciences, Florida Institute of Technology, 150 West University Boulevard, Melbourne, FL 32901; gqin@fit.edu, mzhang@pss.fit.edu, jdwyer@fit.edu, rassoul@pss.fit.edu.

<sup>2</sup> Department of Physics, University of Maryland, College Park, MD 20742; gmmason@umd.edu.

where  $B$  is the averaged background interplanetary magnetic field from the standard Parker spiral (Parker 1958) with the interplanetary magnetic field (IMF) path length to Earth about 1.15 AU for  $V_{sw} = 400 \text{ km s}^{-1}$ , and  $z$  is the coordinate along the magnetic field spiral. In this work we ignore the particles' perpendicular diffusion and adiabatic cooling effects to simplify the condition so that we can concentrate on the effects of pitch angle diffusion models. In addition, we choose a low-energy, short, impulsive event in a case with a large mean free path to help illustrate the effect of model dependence, and since the duration time is short, the adiabatic cooling effects are also smaller. Large particle fluxes in SEP events may generate IMF turbulences so that weak scattering only occurs in small events (Mason et al. 1989). For the complete formula, we should also include these perpendicular diffusion and adiabatic cooling effects (Skilling 1971; Qin et al. 2004). In another paper being prepared we will study the effect of the adiabatic cooling.

If particles are in the isotropic pitch-angle distribution, the parallel mean free path  $\lambda_{\parallel}$  can be written as (Jokipii 1966; Hasselmann & Wibberenz 1968, 1970; Earl 1974)

$$\lambda_{\parallel} = \frac{3v}{8} \int_{-1}^{+1} d\mu \frac{(1 - \mu^2)^2}{D_{\mu\mu}}, \quad (2)$$

or the radial mean free path can be defined as

$$\lambda_r \equiv \lambda_{\parallel} \cos^2 \psi, \quad (3)$$

where  $\psi$  is the angle between radial distance and interplanetary magnetic field.

In order to evaluate equations (1) or (2), the knowledge of the pitch angle diffusion coefficient as a function of  $\mu$ ,  $D_{\mu\mu}(\mu)$ , is essential. In the QLT (Jokipii 1966)  $D_{\mu\mu}$  can be written as

$$D_{\mu\mu} = \frac{1 - \mu^2}{|\mu|v} \frac{Z^2 e^2 V_{sw}}{\gamma^2 m_0^2 c^2} P_{xx} \left( \frac{V_{sw}}{2\pi\mu v} \right), \quad (4)$$

where  $P_{xx}(V_{sw}/2\pi\mu v)$  is the observed power spectrum. In inertial range

$$P_{xx} \propto \mu^q, \quad (5)$$

where  $q > 1$  is the slope of the power spectrum. We can further assume particles have constant radial mean free path,  $\lambda_r$ , propagating through the heliosphere (Bieber et al. 1994). But other theories suggest different forms of the pitch angle diffusion coefficient. Here we follow Beek & Wibberenz (1986) to use an ad hoc model of pitch angle diffusion coefficients

$$D_{\mu\mu}^r \equiv D_{\mu\mu} / \cos^2 \psi = D_0 \left( |\mu|^{q-1} + h \right) (1 - \mu^2), \quad (6)$$

where  $D_0$  is a constant indicating the magnetic field fluctuation level. The constant  $h$  is introduced to help particles transport through  $\mu = 0$  in simulation. A number of theories have been discussed to address particle scattering through  $\mu = 0$  in QLT, e.g., a higher order of corrections to QLT regarding the dissipation range of magnetic fluctuation spectra (Coroniti et al. 1982; Denskat et al. 1983), wave propagation effects (Schlickeiser 1988), and the effects of dynamical turbulence (Bieber & Matthaeus 1991) and thermal wave damping (Achatz et al. 1993; Schlickeiser & Achatz 1993). If nonlinear effects are considered, the transport through  $\mu = 0$  is governed by the level of magnetic fluctuations,

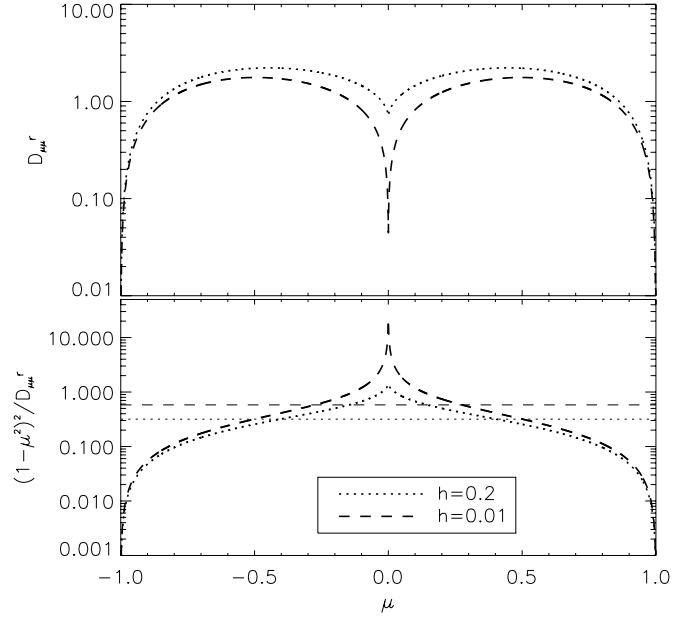


FIG. 1.—Comparison between two models with  $h = 0.2$  (heavy dotted line) and  $h = 0.01$  (heavy dashed line) in arbitrary units. Top:  $D_{\mu\mu}^r$  vs.  $\mu$ . Bottom:  $g(\mu) \equiv (1 - \mu^2)^2 / D_{\mu\mu}^r$  vs.  $\mu$ . The two horizontal lines are the averaged value of  $(1/2) \int_{-1}^1 g(\mu) d\mu$  for  $h = 0.2$  (dotted line) and  $h = 0.01$  (dashed line) models.

i.e.,  $dB/B$  (e.g., Goldstein 1976; Jones et al. 1978; Kaiser et al. 1978; Qin 2002). Recently, Dröge (2003) developed a dynamical QLT model, which has been successfully used to reproduce details of observed particle events, implies resonance broadening effects that can be related to solar wind parameters (magnetic field strength, density, and temperature). The parameter  $h$  could be used as an approximation of the above models and also be related to solar wind observables. If the magnetic spectrum index  $q = 1$ , it is reduced to the isotropic scattering model. For any given model with certain  $q$  and  $h$ , the level of the diffusion can be adjusted by changing the value of  $D_0$ , and thus we can get the best fit of numerical simulations of the transport equation (1) to the observational data. With the value of  $D_0$  for the best fit we go further to calculate the mean free path from equations (2) and (3). This mean free path is called the best-fit mean free path of the observational data.

In this work we use different models of the pitch angle diffusion coefficient to fit an impulsive SEP event observed on 1998 May 16 by the *Wind* STEP instrument. At first, we fix the constant  $q = 5/3$  as the Kolmogorov spectrum and vary  $h$  to obtain models with different scattering levels at  $\mu = 0$ . The two models we consider are with  $h = 0.2$  and  $0.01$ . In Figure 1 the dotted and dashed lines of the top panel shows  $D_{\mu\mu}^r$  versus  $\mu$  from the models with  $h = 0.2$  and  $0.01$ , respectively. From the figure we can see that in both models  $D_{\mu\mu}^r$  reaches its maximum value at the values of  $\mu$  around  $\pm 0.5$ , which is similar to the QLT model ( $h = 0$ ). But in contrast to the QLT models, in these two models  $D_{\mu\mu}^r$  is not zero at  $\mu = 0$  and particles can be scattered through  $90^\circ$ . Note that with the  $h = 0.2$  model,  $D_{\mu\mu}^r$  has a much larger value around  $\mu = 0$ . In § 4 we also show the model dependence of radial mean free path with a series of simulations with different models ( $h, q$ ).

### 3. NUMERICAL METHODS AND RESULTS

In order to solve the focused transport equation (1) we use the Markov stochastic process theory (Zhang 1999, 2000). If we introduce a virtual distribution function  $g(\mu, z, t) \equiv A(z)f(\mu, z, t)$ ,

where  $A(z) \propto 1/B(z)$  is the magnetic flux tube area, the focused transport equation (1) could be written as

$$\begin{aligned} \frac{\partial g}{\partial t} = & -\frac{\partial}{\partial z}(\mu v g) - \frac{\partial}{\partial \mu} \left[ \frac{v}{2L} (1 - \mu^2) + \frac{\partial D_{\mu\mu}}{\partial \mu} \right] g \\ & + \frac{\partial^2}{\partial \mu^2} (D_{\mu\mu} g) + q'(z, \mu, t), \end{aligned} \quad (7)$$

where the virtual source  $q' = Aq$  and the focusing length  $L$  is defined by

$$\frac{1}{L} = -\frac{1}{B} \frac{dB}{dz} = \frac{1}{A} \frac{dA}{dz}. \quad (8)$$

We write the equation in this form because we want to simulate the stochastic particle transport in a time-forward manner. The corresponding time-forward Ito stochastic differential equations may be written as (see Gardiner 1983; Zhang 2000)

$$dz(t) = \mu v dt, \quad (9)$$

$$d\mu(t) = \sqrt{2D_{\mu\mu}} dW_{\mu}(t) + \left[ \frac{v}{2L} (1 - \mu^2) + \frac{\partial D_{\mu\mu}}{\partial \mu} \right] dt, \quad (10)$$

where  $W_{\mu}(t)$  is a Wiener process (e.g., Gardiner 1983). The probability density in the random variable space of  $\{z, \mu\}$  is proportional to the virtual particle distribution function  $g$ , which can be used to further obtain the particle distribution function  $f$  with  $f = g/A$ .

With the two pitch angle diffusion models ( $h = 0.2$  and  $0.01$ ) with  $q = 5/3$ , in § 2 we made the numerical calculation to solve the focused transport equation (1) using the above method. A particle source, which has a rectangular type of release time distribution function with  $\Delta t = 0.03$  days and isotropic initial pitch-angle distribution, is placed at  $r_0 = 0.05$  AU and approximately at 2:30 UT on 1998 May 16. For the short, impulsive, SEP event we study, it is appropriate to assume a nearly point source, which can be confirmed by fitting the anisotropy profiles. The release times match the flare in the *GOES-8* solar X-ray flux profiles whose peak was at 2:00 UT on 1998 May 16.

As a comparison between spacecraft data and simulations with different models, Figure 2 shows time profiles of intensity and anisotropy. Note the anisotropy is in the spacecraft frame. The diamonds (*top panel*) and solid line (*bottom panel*) are from the *Wind* STEP 15 minute average data of 0.31–0.62 MeV nucleon<sup>-1</sup> He. The dotted and dashed lines are from simulations with  $\lambda_r = 1.2$  AU,  $h = 0.2$  and  $\lambda_r = 2.2$  AU,  $h = 0.01$ , respectively. The vertical lines indicate the slightly different releasing times, 2:29:45.6 and 2:39:50.4 UT on 1998 May 16, for simulations with  $\lambda_r = 1.2$  and 2.2 AU, respectively.

The top panel of Figure 2 shows particle intensity versus time. Note that in the intensity profile of the spacecraft data there are short-timescale (3 hr) variations; we assume the “dropouts” are caused by the convection of magnetic flux tubes (Mazur et al. 2000). Here we discarded the three biggest dropouts from the spacecraft data (*filled diamonds*) so that we fit intensity data excluding them. In the top panel for different diffusion models we show the best-fit simulations,  $\lambda_r = 1.2$  AU for  $h = 0.2$  and  $\lambda_r = 2.2$  AU for  $h = 0.01$ . We have simulations (not shown) with small alternations, e.g.,  $\pm 0.2$  AU, that produce unacceptable fits.

The bottom panel of Figure 2 shows the particles’ anisotropy measured in spacecraft frame versus time. The dotted and dashed

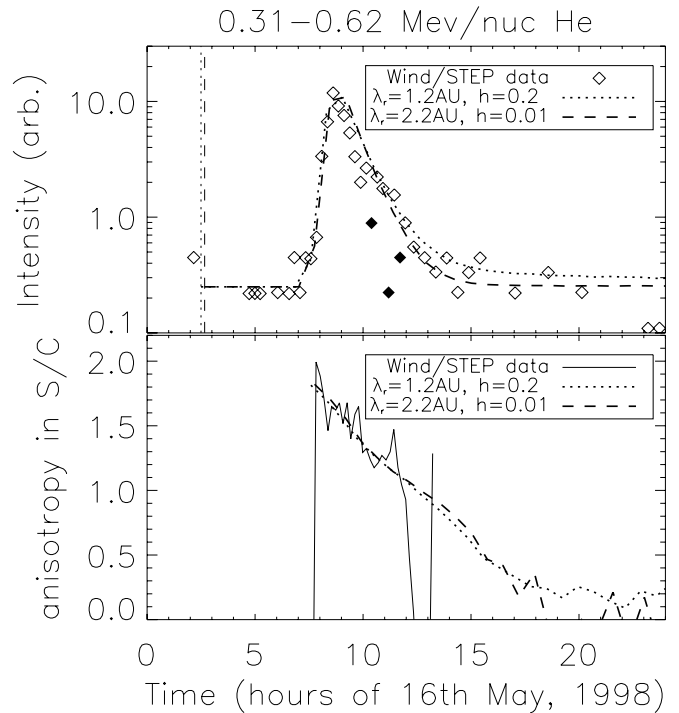


FIG. 2.—Comparison between *Wind* STEP 15 minute average data of 0.31–0.62 MeV nucleon<sup>-1</sup> He (*top*: diamonds, *bottom*: solid line) and simulations (dotted and dashed lines with model parameter  $h = 0.2$  and  $0.01$ , respectively). *Top*: Particle intensity vs. time. Note that the three dropouts are shown as filled diamonds. *Bottom*: Particle first-order anisotropy measured in spacecraft frame vs. time.

lines are from the simulations of best fit in the top panel with model parameter  $h = 0.2$  and 2.2 AU, respectively. We can see before 11 hr (UT) when the particles’ intensity is not too low, both of the profiles of anisotropy of best-fit simulations fit the data well.

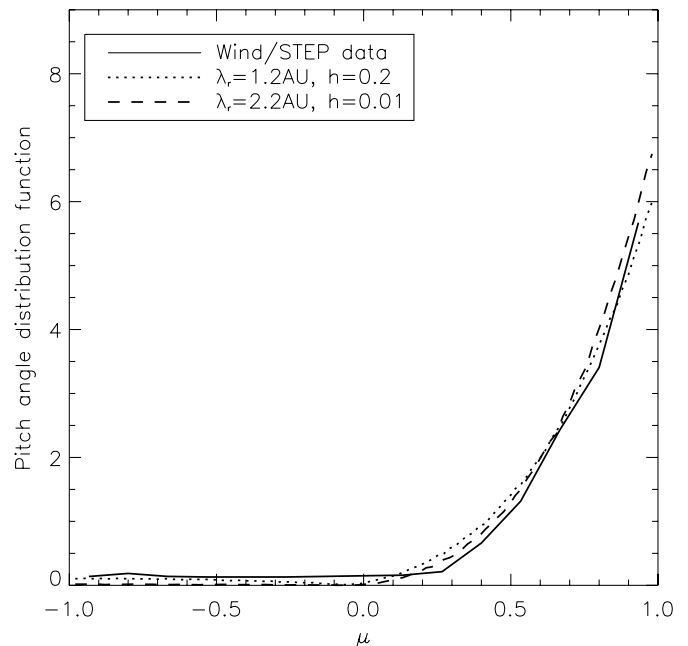


FIG. 3.—Particle cumulative pitch angle distribution function at the position of the satellite for 0.31–0.62 MeV nucleon<sup>-1</sup> He during the period 6:00–15:36 UT on 1998 May 16. The solid line is from the *Wind* STEP observations with eight sectors, and the dotted and dashed lines are from the simulations.

From the two panels of Figure 2, for  $h = 0.2$  and  $0.01$  we obtain mean free paths of  $\lambda_r = 1.2$  and  $2.2$  AU, respectively.

Figure 3 shows the event-averaged particles' pitch angle distribution function from spacecraft observation and simulations detected at the position of the satellite for the SEP event shown in Figure 2 during the period 6:00–15:36 UT on 1998 May 16. We can see that for both of the best-fit simulations with different pitch angle diffusion coefficient models,  $\lambda_r = 1.2$  AU with  $h = 0.2$  and  $\lambda_r = 2.2$  AU with  $h = 0.01$ , the particles have very large anisotropy. Both of the simulation results of the anisotropy agree with spacecraft data, and the difference between the results of the two simulations is not large enough to decide which model of pitch-angle diffusion to be used to compare to the observational data.

#### 4. DISCUSSION

Mean free paths have been widely used to measure the SEPs' pitch-angle diffusion. However, we get different values of the mean free path from the different models of the pitch angle diffusion coefficient  $D_{\mu\mu}$ . In fact, for the definition of equation (2) to be valid, it is required that the particles are nearly isotropic in the pitch-angle distribution, but from Figure 3 we can see that the results from the *Wind* STEP observation and simulations show the particles are not at all in an isotropic distribution. Actually, for the particles in the anisotropic distribution, the effects of  $D_{\mu\mu}$  on the particle transport equation (2) is weighted by the particles' pitch angle distribution function, but in the definition of the mean free path in equation (2) the contribution of different pitch angles is weighted equally.

We can rewrite the definition of the radial mean free path as

$$\lambda_r = (3v/8) \int_{-1}^1 g(\mu) d\mu, \quad (11)$$

where  $g(\mu) = (1 - \mu^2)^2 \cos^2\psi / D_{\mu\mu} = (1 - \mu^2)^2 / D_{\mu\mu}^r$ . The bottom panel of Figure 1 shows  $g(\mu)$  versus  $\mu$  from the two best-fit simulations  $\lambda_r = 1.2$  AU with  $h = 0.2$  and  $\lambda_r = 2.2$  AU with  $h = 0.01$ . The two thin horizontal lines indicate the results of  $(1/2) \int_{-1}^1 g(\mu) d\mu$  for the two models. From the figure we can see that when  $|\mu| \ll 1$ ,  $g(\mu)$  contributes significantly to the results of  $\lambda_r$ , and the difference between the radial mean free paths from the two simulations are mainly from the difference of the integration of  $g(\mu)$  in this range of  $\mu$ . In the simulation with model  $h = 0.2$ , particles scatter more efficiently through  $\mu = 0$  and should return from the antisunward direction easier. By comparing the pitch angle distribution function of models  $h = 0.2$  and  $0.01$  (Fig. 3) we can see that there are more particles with  $\mu < 0$  for the simulation with model  $h = 0.2$ . However, for both of the two models, because the particles are highly anisotropic and more likely to be nearly parallel to the averaged magnetic field, the amount of particles with  $\mu < 0$  is only a very small percentage of the total particles and the time profile of the particles' intensity and anisotropy are mainly determined by the particles nearly parallel to the magnetic field. Since the strength of diffusive scattering of the particles, described by  $D_{\mu\mu} = D_{\mu\mu}^r \cos^2\psi$ , at higher values of  $\mu$  contributes more significantly to the intensity and anisotropy time profile, generally, for each model, we can adjust the constant  $D_0$  to make  $D_{\mu\mu}$  in proper value in a higher range of  $\mu$  to simultaneously fit simulations to the spacecraft data of the time profile of flux and anisotropy. Therefore, in high-anisotropy conditions particle simulations have different best-fit mean free path  $\lambda_r$  described by equation (11).

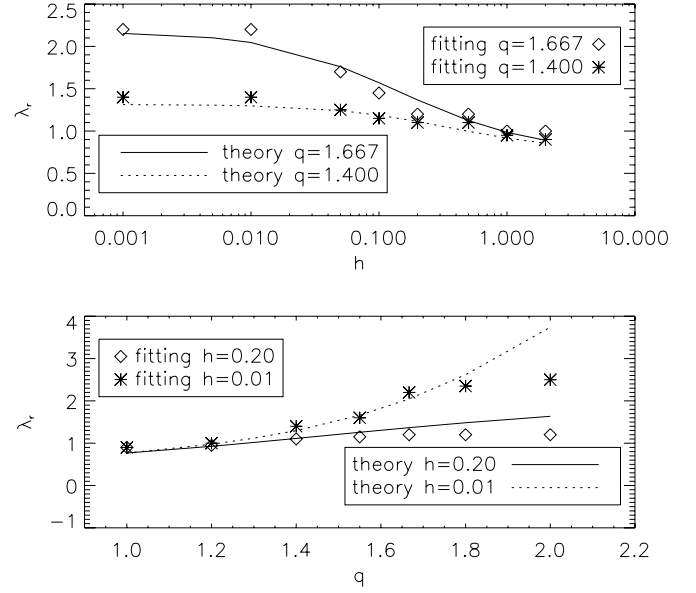


FIG. 4.—Model dependence of radial mean free path  $\lambda_r$ . Top:  $\lambda_r$  vs.  $h$ . Bottom:  $\lambda_r$  vs.  $q$ . Solid and dotted lines are theoretical model calculations for different parameters. Diamonds and asterisks are fittings of simulations to spacecraft data for different parameters.

Furthermore, under the condition  $q \ll 2$  or  $h \gg 0$ , with  $\mu \gg 0$ , and from the definition of the model of pitch angle diffusion coefficients, equation (4) can be written as

$$\frac{\partial D_{\mu\mu} / \partial \mu}{D_{\mu\mu}} = \frac{(q-1)\mu^{q-2}(1-\mu^2) - 2(\mu^{q-1} + h)\mu}{(\mu^{q-1} + h)(1-\mu^2)} \approx -\frac{2\mu}{1-\mu^2}. \quad (12)$$

This means that for higher ranges of  $\mu$ ,  $D_{\mu\mu}$  has the same value for different models fitting the same spacecraft data. Thus, we assume the ad hoc model of the pitch angle diffusion coefficient, equation (4), is

$$D_{\mu\mu} = D_0' D_0'' \left( |\mu|^{q-1} + h \right) (1 - \mu^2), \quad (13)$$

where  $D_0'' = 1/[(\mu_0^{q-1} + h)(1 - \mu_0^2)]$  with a constant for different models  $\mu_0 \gg 0$ , so  $D_{\mu\mu}$  has the same value in a higher  $\mu$  range. We can insert equation (13) into equations (2) and (3) to get a theoretical radial mean free path of each model with only one model-independent free parameter,  $D_0'$ , which can be determined from the fitting results of one simulation to the spacecraft data with any model.

In addition to the two simulations with different models shown above, we obtain a series of radial mean free paths for different models ( $h, q$ ) by fitting simulations to the spacecraft data. Figure 4 shows the model dependence of the radial mean free path  $\lambda_r$ . The top panel shows  $\lambda_r$  versus  $h$ , and the bottom panel shows  $\lambda_r$  versus  $q$ . Diamonds and asterisks are fittings of simulations to spacecraft data. As a reference, theoretical calculation of radial mean free paths with the assumption of equation (13) is also shown as solid and dotted lines for different models. From the figure we can see the fitting results agree with the theoretical calculation very well, except as  $q \rightarrow 2$  in the bottom panel when the conditional equation (12) is invalid. This result demonstrates that under the conditional equation (12) in impulsive SEP events with high anisotropy we only need to fit simulation for one model to the

spacecraft data and we can obtain radial mean free paths for any model by simple theoretical calculations.

From the top panel of Figure 4 we can see that when we fix the parameter  $q$ , the fitted  $\lambda_r$  decreases from its maximum value to the minimum one as  $h$  increases from the limit  $h \rightarrow 0$  to  $h \gtrsim 1$ . On the other hand, the bottom panel shows that when  $q = 1$ , all the models with different  $h$  are reduced to the isotropic scattering one with the minimum value of fitted mean free path  $\lambda_r$ . Furthermore,  $\lambda_r$  increases from its minimum to maximum as  $q$  increases from  $q = 1$  to  $q \gtrsim 2$ . In addition, from the figure we can see that the model dependence of  $q$  is more significant if  $h$  is smaller, unless  $q \gtrsim 2$ , and that the model dependence of  $h$  is more significant if  $q$  is larger.

From the above discussions we conclude that for highly anisotropic particles the value of the pitch angle diffusion coefficient  $D_{\mu\mu}$  in the higher range of  $\mu$  contributes more to the particles' intensity and anisotropy time profile, which can be obtained from the numerical solution of the focused transport equation. Therefore, the mean free path obtained from equations (2) or (3) is not an adequate physical quantity to describe the transport of SEPs. Furthermore, since in such conditions the values of the mean free path obtained from the best fit of the numerical simulations are different with different pitch angle diffusion coefficients models, we cannot even use the parallel mean free path  $\lambda_{\parallel}$  or  $\lambda_r$  defined

with equations (2) or (3), respectively, to indicate the strength of the particles' scattering by the magnetic fluctuations. Instead, we have to use the full definition of the pitch angle diffusion coefficient  $D_{\mu\mu}$ . However, it is a challenge to determine  $D_{\mu\mu}$  from theoretical study or observation.

For example, there are puzzles of some SEP events with abnormally large mean free paths compared to the QLT results from magnetic field power spectra (e.g., Tan & Mason 1993). These might, in part, relate to the difficulty of the lack of knowledge of  $D_{\mu\mu}$  for the large anisotropic case. Generally, we cannot easily get the accurate  $D_{\mu\mu}$  function to numerically solve the focused transport equation. Therefore, in high-anisotropy cases, if we practically still report the value of the large mean free path as a crude measure of the relative scattering conditions between different SEP events or different species, at least the model of diffusion coefficients used should also be shown.

The authors benefited from the *Wind* SWE data provided by K. W. Ogilvie, R. B. Torbert, and A. J. Lazarus and the *Wind* MFI data provided by R. P. Lepping. This work was supported partly by NASA grants NAG5-11036, NAG5-13514, NAG5-11921, NSF SHINE grant 0203252, and JPL contract 1240373.

#### REFERENCES

- Achatz, U., Dröge, W., Schlickeiser, R., & Wibberenz, G. 1993, *J. Geophys. Res.*, 98, 13261
- Beeck, J., & Wibberenz, G. 1986, *ApJ*, 311, 437
- Bieber, J. W., & Matthaeus, W. H. 1991, *Proc. 22nd Int. Cosmic Ray Conf.*, Vol. 3, ed. M. Cawley et al. (Dublin: Dublin Inst. Adv. Stud.), 248
- Bieber, J. W., Matthaeus, W. H., Smith, C. W., Wanner, W., Kallenrode, M.-B., & Wibberenz, G. 1994, *ApJ*, 420, 294
- Coroniti, F. V., Kennel, C. F., Scarf, F. L., & Smith, E. J. 1982, *J. Geophys. Res.*, 87, 6029
- Denskat, K. U., Beinroth, H. J., & Neubauer, F. M. 1983, *J. Geophys.*, 54, 60
- Dröge, W. 2003, *ApJ*, 589, 1027
- Dwyer, J. R., Mason, G. M., Mazur, J. E., Jokipii, J. R., von Rosenvinge, T. T., & Lepping, R. P. 1997, *ApJ*, 490, L115
- Earl, J. A. 1974, *ApJ*, 193, 231
- Gardiner, C. W. 1983, *Handbook of Stochastic Methods for Physics, Chemistry, and the Natural Sciences* (Berlin: Springer)
- Goldstein, M. L. 1976, *ApJ*, 204, 900
- Hasselmann, K., & Wibberenz, G. 1968, *Z. Geophys.*, 34, 353
- . 1970, *ApJ*, 162, 1049
- Jokipii, J. R. 1966, *ApJ*, 146, 480
- Jones, F., Birmingham, T. J., & Kaiser, T. B. 1978, *Phys. Fluids*, 21, 347
- Kaiser, T. B., Birmingham, T. J., & Jones, F. 1978, *Phys. Fluids*, 21, 361
- Kocharov, L., Vainio, R., Kovaltsov, G. A., & Torsti, J. 1998, *Sol. Phys.*, 182, 195
- Lepping, R. P., et al. 1995, *Space Sci. Rev.*, 71, 207
- Mason, G. M., Ng, C. K., Klecker, B., & Green, G. 1989, *ApJ*, 339, 529
- Mazur, J. E., Mason, G. M., Dwyer, J. R., Giacalone, J., Jokipii, J. R., & Stone, E. C. 2000, *ApJ*, 532, L79
- Ng, C. K., & Reames, C. K. 1994, *ApJ*, 424, 1032
- Ng, C. K., & Wong, K. Y. 1979, *Proc. 16th Internat. Cosmic Ray Conf.*, Vol. 5, ed. S. Miyake (Tokyo: Univ. Tokyo Press), 252
- Ogilvie, K. W., et al. 1995, *Space Sci. Rev.*, 71, 55
- Parker, E. N. 1958, *ApJ*, 128, 664
- . 1963, *Interplanetary Dynamical Processes* (New York: Interscience)
- . 1965, *Planet. Space Sci.*, 13, 9
- Qin, G. 2002, Ph.D. thesis, Univ. Delaware
- Qin, G., Zhang, M., Dwyer, J. R., & Rassoul, H. K. 2004, *ApJ*, 609, 1076
- Roelof, E. C. 1969, in *Lectures in High Energy Astrophysics*, ed. H. Ögelman & J. R. Wayland (NASA SP-199; Washington: NASA), 111
- Ruffolo, D. 1991, *ApJ*, 382, 688
- Schlickeiser, R. 1988, *J. Geophys. Res.*, 93, 2725
- Schlickeiser, R., & Achatz, U. 1993, *J. Plasma Phys.*, 49, 63
- Schlüter, W. 1985, Ph.D. thesis, Univ. Kiel
- Schulze, B. M., Richter, A. K., & Wibberenz, G. 1977, *Solar Phys.*, 54, 207
- Skilling, J. 1971, *ApJ*, 170, 265
- Tan, L. C., & Mason, G. M. 1993, *ApJ*, 409, L29
- Torsti, J., Riihonen, E., & Kocharov, L. 2004, *ApJ*, 600, L83
- von Rosenvinge, T. T., et al. 1995, *Space Sci. Rev.*, 71, 155
- Zhang, M. 1999, *ApJ*, 513, 409
- . 2000, *ApJ*, 541, 428